the plant journal

SEB SOCIETY FOR EXPERIMENTAL BIOLOGY

The Plant Journal (2025) **123,** e70409 doi: 10.1111/tpj.70409

Rooting mechanism of *Dendrocalamus brandisii* branch and main differences in rooting ability in three different bamboo species

Lixia Yu[1,2,3], Hui Zhan[1,2], Caihua Chu[3], Diankun Jin[3], Lingfeng Li[1,2], Juan Li[1,2,3], Changming Wang[1,2], Todd F. Shupe[4] and Shuguang Wang[1,2,*]

[1]*Biological Research and Utilization Innovation Team in Bamboo Resources of Yunnan Province, Southwest Forestry University, Kunming, China,*

[2]*Key Laboratory of Forest Resources Conservation and Utilization in the Southwest Mountains of China, Ministry of Education, Southwest Forestry University, Kunming, China,*

[3]*College of Biological Science and Food Engineering, Southwest Forestry University, Kunming, China, and*

[4]*School of Renewable Natural Resource, Louisiana State University Agricultural Center, Baton Rouge, Louisiana, USA*

Received 20 March 2025; revised 16 July 2025; accepted 21 July 2025.
*For correspondence (e-mail stevenwang1979@126.com).

SUMMARY

Adventitious root (AR) growth is vital for mass propagation of bamboo, and there is a significant difference in the rooting ability among different bamboo species. The differences of AR differentiation from the bamboo branch were undefined. In this study, it was found that the thickness and lignification degrees of the cortex were closely related to the degree of rooting difficulty of the branch base in different bamboo species. The inner cortical cells restored their division ability and further differentiated AR primordium in *Dendrocalamus brandisii*. Indole-3-acetic acid (IAA) and jasmonic acid (JA) played a crucial role in the development of ARs, and further IAA and JA treatment analysis indicated that only low concentration hormones could enhance AR differentiation. *DbCRL1* and *DbAOS1* were defined to be related to the AR differentiation, and their positive functions were validated in rice. *DbAOS1* exhibited an ability to independently enhance and activate *ANTHRANILATE SYNTHASE* in the auxin production pathway. *DbCRL1* could interact with *DbWOX11 in vivo* and *in vitro*, wherein they promote AR differentiation synergistically. These findings revealed the differences of AR differentiation in the branch and provided new insights into the rooting mechanism of *D. brandisii* branch.

Keywords: rooting ability, adventitious root differentiation, indole-3-acetic acid, jasmonic acid.

INTRODUCTION

Bamboos belong to the grass family and have enormous economic, ecological, and social ramifications globally (Chaturvedi et al., 2023). Compared with crops or economic trees, bamboos bloom infrequently and exhibit a low seed setting rate. Consequently, vegetative propagation is widely used for afforestation, with adventitious roots (ARs) differentiation playing a crucial role in this process. Vegetative propagation varies among different types of bamboo due to their significant differences in rooting ability (Singh et al., 2013). Our observations on *Dendrocalamus brandisii* showed that there are ARs in the base and lower nodes of bamboo culms (3–4 nodes above the ground), and even the branch base can produce roots under the environmental conditions of high humidity and high temperature in the rainy season (Chu et al., 2020). These branches can develop into new plants after cutting, and accordingly, the culms and nodes are usually selected for branch cuttage. However, the bamboo species of *Fargesia*, such as *Fargesia yunnanensis*, are unable to produce root primordium at the base of their branches in natural environments. One of our previous studies also showed only a few ARs can be induced from their branch bases after 1 year via the method of trenching layering with culm bases (Wang et al., 2010). Moreover, the branch bases of the scattered bamboos, including *Phyllostachys edulis* and *Phyllostachys mannii*, lack root primordium in natural environments and even under cuttings. The differentiation capabilities of ARs vary significantly among different bamboo species. What causes the difference in ARs differentiation ability is unknown.

The formation of ARs varies with species and original positions. ARs usually emerge from the non-root tissue

and are formed upon wounding or other types of abiotic stress (Zeng et al., 2021). ARs can be formed directly from leaves or stems in some plants (Fattorini et al., 2018), or directly from callus (Verstraeten et al., 2014). Many plant species are able to regenerate ARs from aerial parts or tissues that undergo excessive proliferation (Jing et al., 2020). Some species have a single origin of root primordia. By definition, ARs originate from dormant preformed meristems, or from cells neighboring vascular tissues in stems or leaves (Joshi & Ginzberg, 2021). In rice, AR formation includes three key stages: the emergence of founder cells from cells adjacent to the vascular cylinder, the initiation and differentiation of root primordia, and the emergence of AR. This process is crucial for the plant's ability to absorb nutrients and water, and it is influenced by various factors including hormones and environmental conditions (Singh et al., 2023). The origination position of AR primordium in the branch base of *D. brandisii* has not been determined.

The regulation of AR formation is an adaptive response to different environments (Atkinson et al., 2014; Bellini et al., 2014; Gonin et al., 2019). In wheat (*Triticum aestivum*), waterlogging induces the formation of nodal roots with aerenchyma tissues (Nguyen et al., 2018), a process facilitated by the production of ethylene and reactive oxygen species. These signaling molecules enhance the expression of genes involved in auxin biosynthesis and transport, thereby promoting the emergence of nodal roots (Nguyen et al., 2018; Yamauchi et al., 2014). Low-oxygen conditions might directly regulate the reactivation of dormant AR primordia in the submerged stems. The overexpression of the *ZmEREB180* gene was found to significantly enhance crown root (CR) initiation in maize under waterlogged conditions (Yu et al., 2019). The WUSCHEL-related homeobox (WOX) and lateral organ boundaries domain transcription factor families play essential roles in controlling CR development in rice (Geng et al., 2024). Additionally, mineral deficiency can also increase AR formation. Under conditions of nitrogen, phosphorus, potassium, and sulfur deficiencies, *OsmiR167* in rice targets and degrades *OsARF8*, thereby reducing the function of *OsGH3.2* and increasing the levels of active auxin in roots, which may indirectly enhance CR formation in rice (Grewal et al., 2018). Unlike some model plants, ARs originate post-embryonically from tissues, which may occur in response to flooding, darkness, nutrient deprivation, or mechanical wounding (Lakehal & Bellini, 2019; Steffens & Rasmussen, 2016). As monocotyledonous plants, bamboo lacks a lateral meristem, with height growth mainly depending on the intercalary meristem. There is limited research on the regulation of AR formation in bamboo. The root primordium differentiation mechanism is also unclear.

Root regeneration initiates in the distal root meristem formation, followed by the activation of a stem cell niche, and cell identity is closely correlated with hormone domain formation (Efroni et al., 2016; Gonin et al., 2019; Lakehal & Bellini, 2019). The acquisition of specific cells of plants primarily relies on the regulated orientation of cell divisions (Rasmussen & Bellinger, 2018). However, the signals and mechanisms governing the transition between cell-cycle stages and the regulation of the cell division plane during patterning are presumably plant specific (Marhava et al., 2019). What accounts for the variations in ARs differentiation ability among different bamboo species? Systematic investigations into the molecular and physiological mechanisms underlying ARs differentiation are lacking. In this research, the anatomy, physiology, and multi-omics methods were employed to solve the problem. The structural characteristics and differentially expressed genes (DEGs) expression of three types of bamboos, including *D. brandisii, F. yunnanensis*, and *P. mannii*, were analyzed, and the dynamical changes in sugar metabolism and hormones were also investigated during ARs differentiation. Gene modules were derived from the weighted correlation network analysis (WGCNA) based on Kyoto Encyclopedia of Genes and Genomes (KEGG) pathways. The functional hormones and genes were filtered and verified, and the physiological differences and the related gene expression pattern were analyzed. By conducting a comprehensive analysis of ARs differentiation, a global architecture of the positive regulator in bamboo root induction was established. Our study demonstrated the differences in AR differentiation in branches among different bamboo species and revealed the potential mechanism underlying AR formation in easily rooted bamboo species.

RESULTS

Morphological and anatomical differences in the branch bases of different bamboo species

There were significant morphological and anatomical differences in the branch bases of *D. brandisii*, *F. yunnanensis*, and *P. mannii* (Figure 1a–c). The branch bases of *D. brandisii* exhibited significant swelling and more pronounced nodes compared to those of *F. yunnanensis* and *P. mannii*. ARs usually formed at the position close to the sheath scar. The branch bases of *F. yunnanensis* and *P. mannii* showed higher lignification of epidermis compared to those of *D. brandisii* (Figure 1d–f). It could also be noticed that the density of vascular bundles in the cortex increased with the increasing difficulty of rooting in the branch bases of *F. yunnanensis* and *P. mannii* (Figure 1e,f). The bamboos with intensive nodes, lower lignification of epidermis, and thicker cortex and subcutaneous layer at the branch bases showed a higher ability in AR differentiation as compared to those of the bamboos with longer internodes, higher lignification of epidermis, and thicker cortex and subcutaneous layer at the branch bases. Higher lignification, thinner cortex, and subcutaneous layer in the

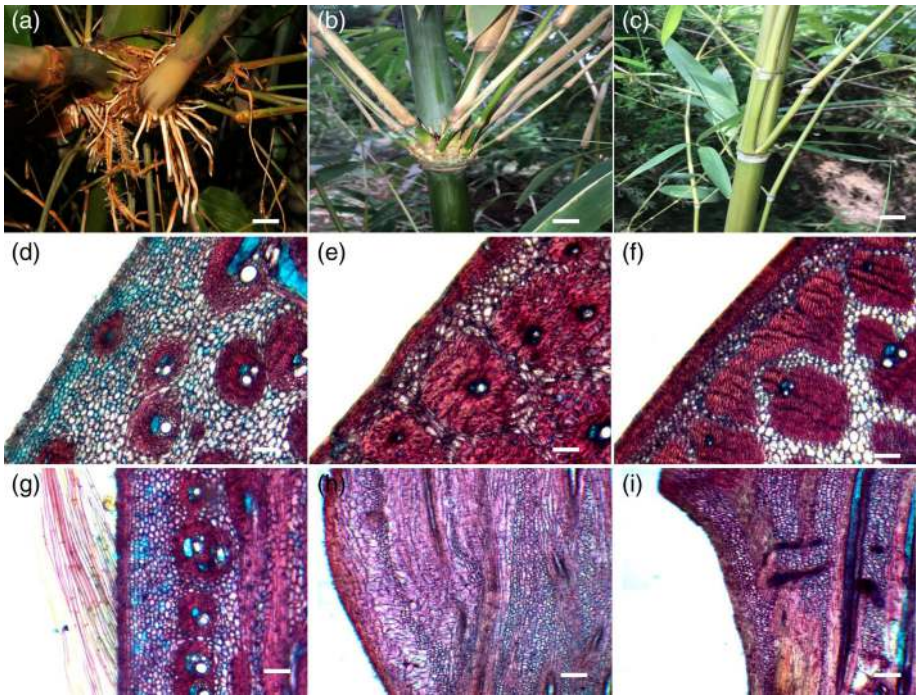

Figure 1. Morphological and anatomical differences of the branch base in different bamboo species.
(a–c) Morphology of the branch base in *Dendrocalamus brandisii*, *Fargesia yunnanensis*, and *Phyllostachys mannii*, respectively. Scale bar, 4 cm. The branch bases of *D. brandisii* exhibited significant swelling and more pronounced nodes compared to those of *F. yunnanensis* and *P. mannii*. Only a few nodes could be observed in the branch bases of *F. yunnanensis*, and no apparent nodes were observed in the branch bases of *P. mannii*.
(d–f) Anatomical structure of cross section of the branch base in *D. brandisii, F. yunnanensis*, and *P. mannii*, respectively. Scale bar, 200 μm. The branch bases of *F. yunnanensis* and *P. mannii* showed higher lignification of epidermis compared to those of *D. brandisii*. The density of vascular bundles in the cortex increased with the increasing difficulty of rooting; this limited their secondary meristematic cells formation and root primordium regeneration in the branch bases of *F. yunnanensis* and *P. mannii*.
(g–i) Anatomical structure of longitudinal section of the branch base in *D. brandisii, F. yunnanensis*, and *P. mannii*, respectively. Scale bar, 200 μm. Lower lignified degree and more parenchyma cells in the cortex were observed; more transverse vascular bundles were found in *D. brandisii* compared to *F. yunnanensis* and *P. mannii*.

branch bases of *F. yunnanensis* and *P. mannii* limited the secondary meristematic cell formation and root primordium differentiation. These results indicated that the AR differentiation capacity of the branch bases in different bamboo types depended highly on the morphological and anatomical characteristics of the branch bases.

According to the changes in morphological and anatomical structural characteristics of the branch bases of *D. brandisii*, the ARs differentiation could be divided into four stages, that is, stage I, II, III, and IV, separately (Figure 2). The root primordia usually began their differentiation at the young and tender stage of branch bases (Figure 2a–c, e–g). Parenchyma cells in the inner part of the cortex and close to the outer vascular bundles of the branch bases restored their differentiation ability (Figure 2i,m,q–t) and differentiated into a new root apical meristem via continuous mitosis (Figure 2j,n), which finally bulged outward to form the root primordium (Figure 2j,k). In the branch bases of *D. brandisii*, the root primordium originated from the inner cortex cells that were close to the outer vascular bundles, which restored their ability to differentiate. What's more, the differentiation of ARs from the branch bases of *D. brandisii* was endogenous in origin.

Physiological changes in sugar metabolism and endogenous hormone contents during ARs differentiation in the branch bases of *D. brandisii*

Sugar metabolism played important roles in the AR differentiation of *D. brandisii*. The changes in endogenous starch contents and soluble sugar contents showed an opposite trend from stage I to stage III, and they increased significantly in stage IV (Figure S1A–E). The non-structural carbohydrates (NSC) maintained a relatively stable level in the first three stages and increased significantly in stage IV (Figure S1F). The activities of the related metabolizing enzymes also changed accordingly. In the synthesis direction of starch, soluble starch synthases (SSS) and granules bound starch synthases (GBSS) activities had a similar trend to that of starch content (Figure S1G,H). The degradation direction of starch enzymes, including the ADP-glucose pyrophosphorylase (AGPase) and starch phosphorylase (STP) activities, were rather high and

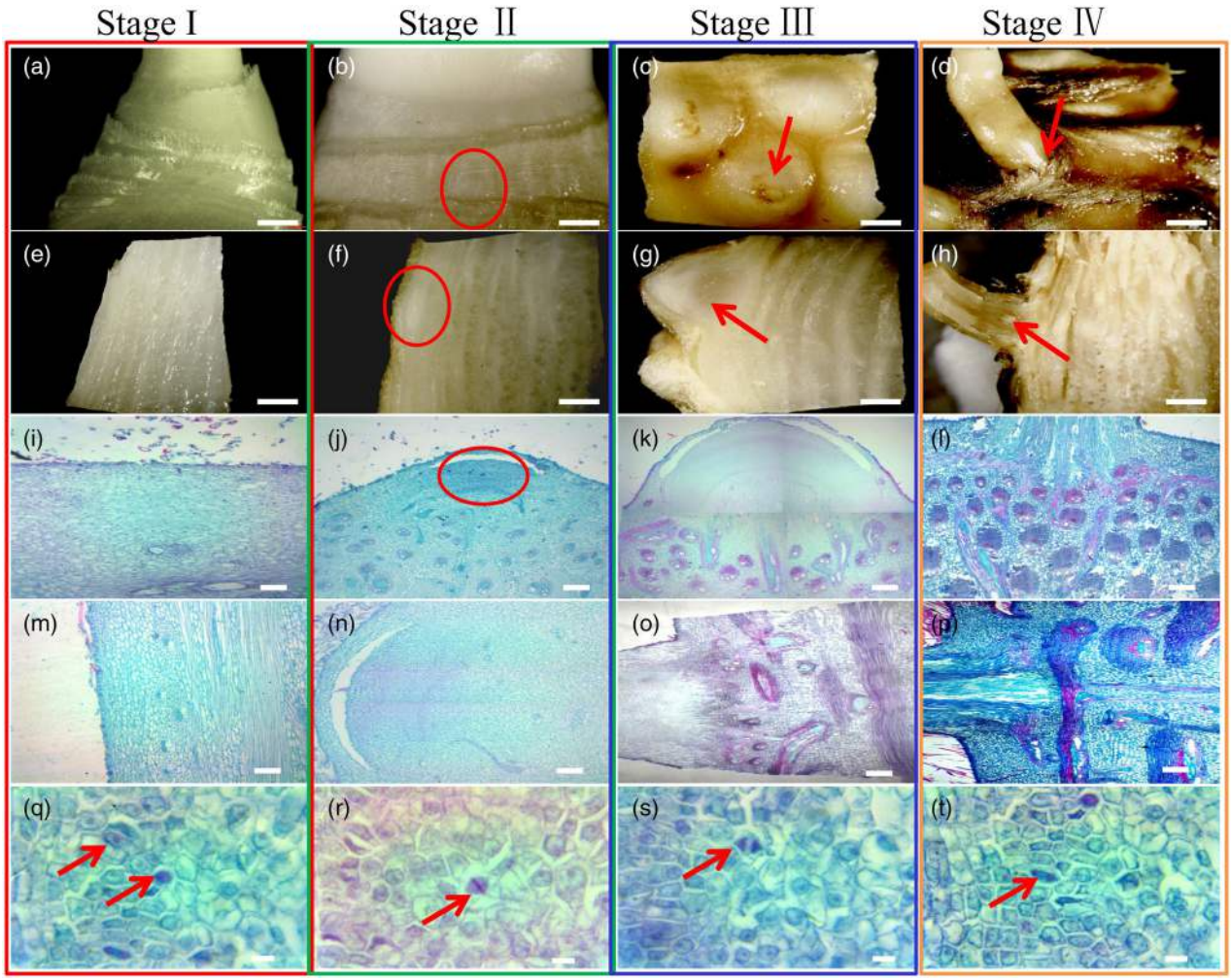

Figure 2. Morphological and anatomical differences of the branch base during adventitious roots (ARs) differentiation in *Dendrocalamus brandisii*.
(a–h) Morphology of the branch base in different ARs development stages. Scale bar, 2 mm. Four stages, including stage I, II, III, and IV, were divided. With the ARs differentiation, the bulges were more and more obvious, and the root was formed in stage IV. Stage I (0 day): Roots undifferentiated, cortical cells in a quiescent state; Stage II (2 days): Inner cortical cells regain division ability, initiating root primordium formation; Stage III (3 days): Root primordium structure formed, with continuous cell proliferation; Stage IV (7 days): ARs break through the epidermis, completing morphogenesis.
(i–l) Anatomical structure of the branch base in different ARs development stages (cross section). Scale bar, 100 μm. The root primordia became more and more prominent with the development of the branch base. Finally, the root primordium continued to elongate and finally broke out of the epidermis and formed a complete root.
(m–p) Anatomical structure of the branch base in different ARs development stages (longitudinal section). Scale bar, 200 μm. The parenchyma cells close to the vascular bundles differentiated into new radial vascular cells that connected inwardly and transversely with the outer vascular bundles of branch bases.
(q–t) Cell mitosis of the branch base in different ARs development stages. Scale bar, 50 μm.

increased constantly (Figure S1I,J). Vacuolar invertase (VIN) showed much higher activity values as compared to soluble acid invertase (SAI), cell wall-bound acid invertase (CWI), and sucrose synthase (SUSY) (Figure S1K–N), which implied that VIN played a more vital role in AR differentiation. The cellulose content also showed an upward trend (Figure S1O). These results demonstrated that there were constant transformations among the substances, including starch, soluble sugar, and cellulose. Sugar metabolism was quite active, and more cellulose was synthesized during AR differentiation. A large amount of carbohydrates was consumed during AR differentiation, especially at the root primordium initiation stage, by increasing the activities of sucrose metabolizing enzymes and the expression levels of the related genes during AR development.

The content of indole-3-acetic acid (IAA) increased from stage I to stage II and then decreased sharply (Figure S2A), which implied that IAA was a key response factor for the initiation of root primordium. The content of other auxin hormones, such as ICA, ICAld, and ME-IAA, was relatively low (Figure S2B–D). The cytokinins contents showed a decreasing trend and maintained a low level during the whole root differentiation process (Figure S2E–G). The ratio of IAA to tZ increased first and then decreased in

the subsequent stages (Figure S2H). The trend of changes in jasmonic acid (JA) content was similar to IAA (Figure S2I), which indicated that JA might play positive functions in AR differentiation. JA-ILE content also increased gradually during root differentiation, but its content was much lower than that of JA (Figure S2J). As for SA, it sharply dropped from stage I to stage II and then increased continuously in the subsequent two stages (Figure S2K). This implied that a high concentration of SA did not play the key roles in the differentiation of root primordium. ABA showed a constantly decreasing trend, implying its negative effects on AR differentiation (Figure S2L). The results indicated that IAA and JA were crucial for AR differentiation.

Dynamics changes in metabolites in the branch bases of *D. brandisii*

Compared with those in stage I, a total of 129 metabolites, including 68 upregulated and 61 downregulated, were observed in stage II. Fer-agmatine, Hispidulin, Tricin O-feruloylhexoside O-hexoside, and Catechin gallate et al. were significantly enriched in stage I/II specially (Figure S3A). The differentially accumulating metabolites (DAMs) mainly consisted of amino acids, sugars, and flavonoids, with a notable subset being linoleic acids. As a precursor substance of JA, these acids included four upregulated metabolites and one downregulated metabolite, which was specially accumulated in stage I/II (Figure S3B). Compared with stage I/II, there were more DAMs in stage II/III and stage III/IV (Figure S3C–F), which indicated that more substances were prepared for AR development.

RNA-seq and DEGs analysis in branch bases of different bamboo species during ARs differentiation

The branch bases of *D. brandisii*, *F. yunnanensis*, and *P. mannii* were selected at different developmental stage (Figure 3), and mRNA-Seq was performed from cortex tissues (Dataset S1–S3). The gene expression difference among different developmental stages in the three bamboo speices were analyzed using principal component analysis (PCA) and Venn diagram (Figure 3a–d). Similar to the changes of DAMs, the number of DEGs increased with AR development in *D. brandisii* (Figure 3b). In all of three bamboo species, the number of the upregulated genes (2398, 2349, 5461 in *D. brandisii, F. yunnanensis* and *P. mannii*, respectively) was more than that of the downregulated genes (1586, 1940, 4613 in *D. brandisii, F. yunnanensis* and *P. mannii*, respectively) with their branches development (Figure 3e). The number of DEGs related to IAA synthesis, cellulose synthase and sugar metabolism in *D. brandisii* was more than those of *F. yunnanensis* and *P. mannii* (Figure 3g). Comparing to *F. yunnanensis* (Figure S4A) and *P. mannii* (Figure S4B), *D. brandisii* exhibited a more active molecular function, with the majority of DEGs categorized under 'cellulose synthesis activity', 'glutathione transferase activity', and 'MAP kinase activity' (Figure S5A–G). Accordingly, these DEGs might play an important role in AR differentiation, which might be affected by many factors such as hormone-mediated signaling pathway and cellulose biosynthesis. The result of quantitative reverse transcriptase-polymerase chain reaction (qRT-PCR) in the branch base of *D. brandisii* was consistent with the trend of transcriptome (Figure S6), in which each sample had three biological replicates and three technical replicates to meet the requirements for data reliability.

Sucrose metabolism and phytohormone regulation pathway based on correlation analysis

The co-joint KEGG pathway enrichment analysis revealed that the metabolic pathways, including the biosynthesis of secondary metabolites, phenylpropanoid biosynthesis, starch and sucrose metabolism, and biosynthesis of amino acids, were highly enriched and consistent across stage I/II and III/IV (Figure S7A,B). In the starch and sucrose metabolism pathway (Figure 4), invertase (*INV*), and *SUSY* played a pivotal role in deposing sucrose. As the most abundant storage carbohydrate, starch degradation and synthesis in plastids depended mainly on alpha-amylase (*AMY*), beta-amylase (*BMY*), isoamylase 3 (*ISO3*), and 1,4-alpha-glucan-branching enzyme (*GBE1*). Consistent with the physiological changes in starch and sucrose metabolism, the expression of genes was consistent with the degradation of starch and sucrose during AR differentiation.

As shown in Figure S7C,D, the number of genes involved in the pathways of IAA and JA biosynthesis and metabolism increased during AR differentiation. The *TAA* and *YUC* genes were upregulated significantly during the AR initiation stage. *AUX/IAA* and *GH* genes were significantly upregulated in stage I/II, and the auxin efflux carrier (*PIN*) was downregulated. The lipoxygenase (*LOX*) and allene oxide synthase (*AOS*) genes and the precursor substances of JA synthesis, including α-linolenic acid, 13-HPOT, and 12, 13-EOT, were upregulated significantly during AR differentiation. Negative regulatory factors of JA, including *COI1*, *JAZ*, and *MYC2*, were downregulated in stage IV. The expression of JASMONATE RESISTANT 1 (*JAR1*, encoding a JA-conjugating enzyme) fluctuated during AR differentiation. An enhancement in *ANTHRANILATE SYNTHASE* (*ASA1*) expression was observed during AR differentiation. These results revealed that the expression of genes in IAA and JA biosynthesis was consistent with the accumulation of phytohormones and related metabolites (Figure 5).

Effects of exogenous IAA and JA on ARs formation in the cuttage and tissue culture plantlets of *D. brandisii*

Compared to the control, there were noticeably more ARs after applying a lower concentration of exogenous

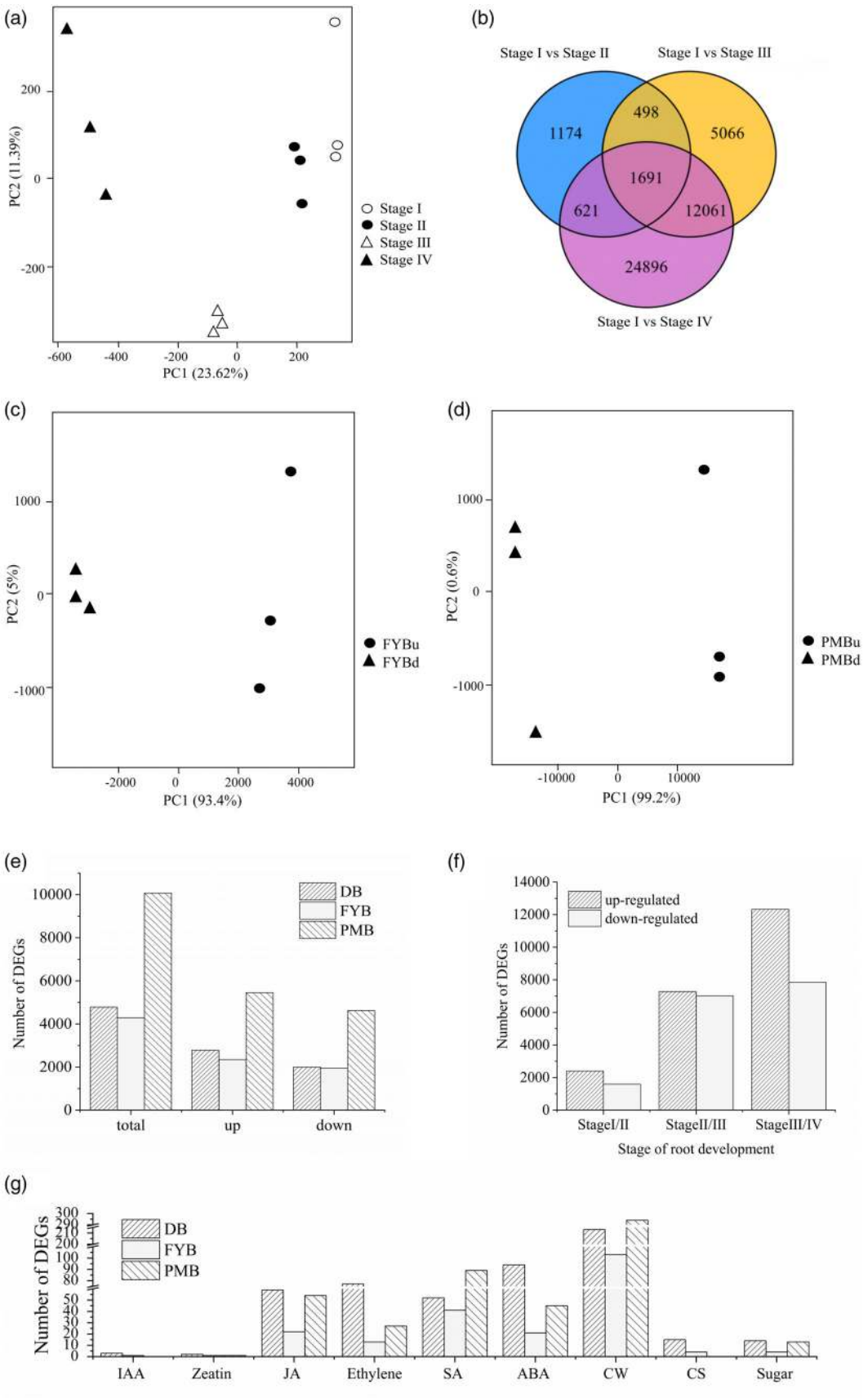

Figure 3. Genotype influence on the bamboo transcriptome during different developmental stage.
(a) Principal component analysis (PCA) of the branch base in *Dendrocalamus brandisii* during root differentiation.
(b) Venn diagram depicting the overlapping differentially expressed genes (DEGs) between developmental stages of *D. brandisii*.
(c, d) PCA of the branch base in *Fargesia yunnanensis* and *Phyllostachys mannii*, respectively.
(e–g) Bar plots representing numbers of DEGs at different developmental stages in different bamboo species.

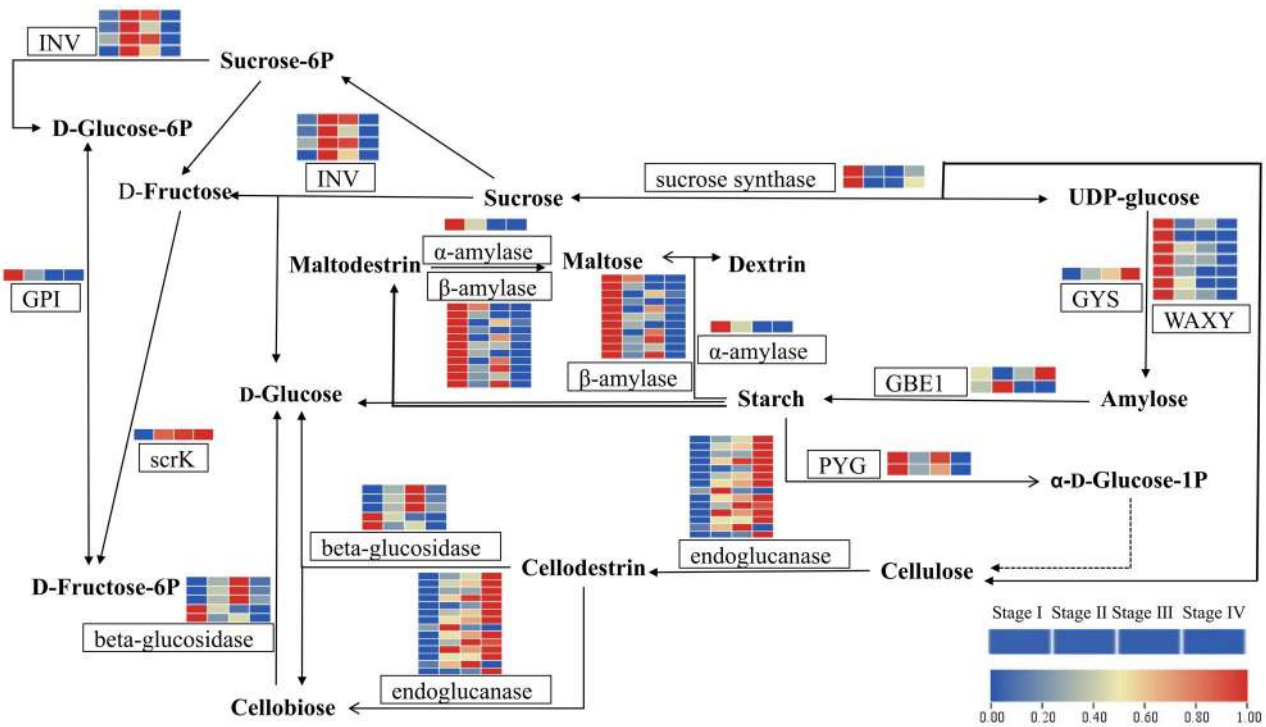

Figure 4. Starch and sucrose metabolism pathway regulating adventitious root differentiation of *Dendrocalamus brandisii*.
The metabolites are regulated by genes (rectangle box). Red represents up regulation; green means down regulation; blue indicates both up and down regulations.

hormones 30 days post-cutting (Figure S8A–C). The rooting rate, number, and length increased and then decreased as the hormone concentrations increased (Figure S8D–F). No statistically significant difference was found in total root length between treatments with IAA and JA (Figure S8E). Furthermore, the morphology of ARs treated by JA was shorter and thicker than those of IAA and the control. These results suggested that both IAA and JA promoted AR differentiation, whereas their roles were not completely the same in root architecture establishment. The morphological characteristics of the ARs from the tissue culture seedlings confirmed the positive role of IAA and JA in AR differentiation (Figure S9). Compared with the control (Figure S9A,E), a lower concentration of IAA and JA (10 μM) could enhance AR formation effectively (Figure S9B,F), whereas a higher concentration of IAA and JA (20 and 30 μM) was found to inhibit AR formation apparently (Figure S9C,D,G,H).

Influence of exogenous IAA and JA on the sugar metabolism and endogenous hormones during ARs formation in the branch bases of *D. brandisii*

After the application of both IAA and JA, the endogenous soluble sugar content of the branch bases increased gradually, with the highest content at 36 h (Figure S10A), which was close to that in the branch bases at stage I. Similarly, the activities of VIN, CWI, and SUSY showed a gradually increasing trend with time (Figure S10B–D). However, the values of those treated with JA were always lower than those of branches treated with IAA but were higher than those of the control. The starch content also showed an increasing trend, except for that treated with IAA at 36 h, which decreased slightly (Figure S10E). The activities of enzymes related to starch synthesis, including SSS, GBSS, and AGP, decreased constantly except for the STP (Figure S10F–I). The NSCs contents also showed an increasing trend with time (Figure S10J). These results

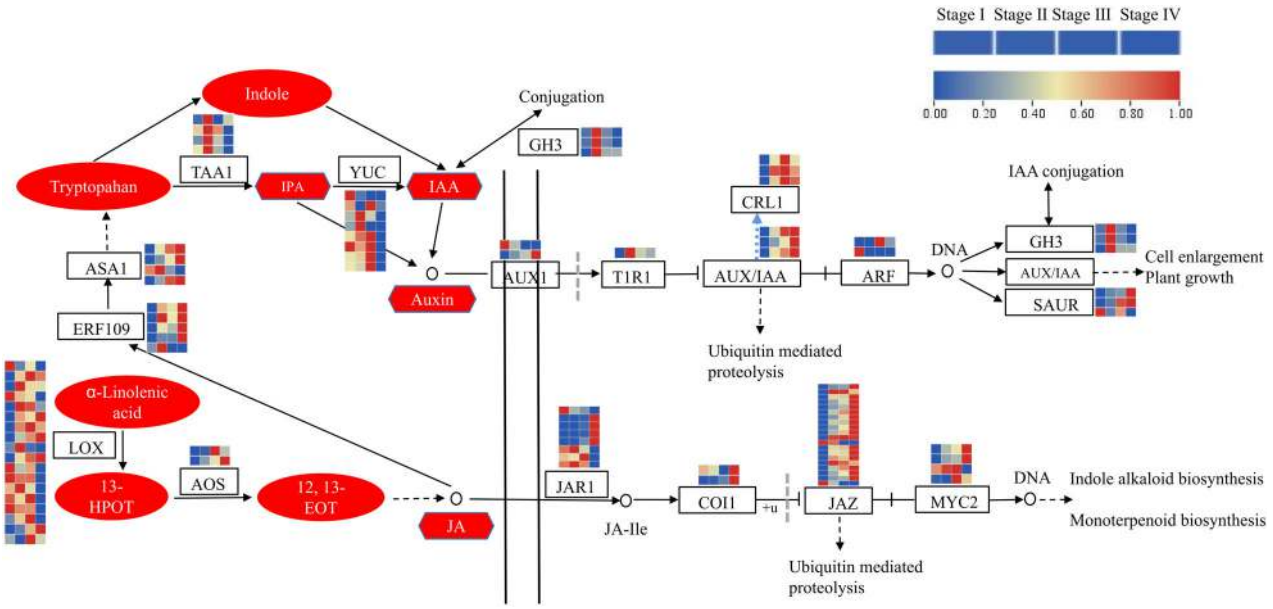

Figure 5. The structural architecture of the regulation between IAA and JA in adventitious roots development.
The metabolites (oval box) can affect the biosynthesis of hormones (hexagon box), which processes are regulated by genes (rectangle box). Red represents up regulation, green means down regulation, and blue indicates both up and down regulations.

confirmed that both the exogenous JAA and JA could enhance the AR initiation.

The content of endogenous IAA increased significantly no matter under the exogenous JA or IAA treatment as compared to the control (Figure S10K). The tZ content decreased gradually (Figure S10L). The increased ratio of IAA to tZ was similar to that at the AR primordium initiation stage. Additionally, the JA content also reached the peak in 36 h after the exogenous IAA treatment (Figure S10M), implying that there was a mutually promoting relationship between the synthesis of IAA and JA, and both of which played an important role in ARs differentiation.

Gene expression related to root differentiation in the branch bases after the exogenous IAA and JA application

To investigate the molecular mechanism of hormonal regulation in ARs differentiation and development, the modulation in global architecture of gene expression was studied by analyzing the genes whose expression levels were changed after the exogenous IAA and JA treatments in the cortex of branch bases (Figure S11; Dataset S4). The gene expression variation across treatments was analyzed through PCA (Figure S11A). IAA treatment significantly enhanced the expression levels of DEGs, with a notable predominance of upregulated genes over downregulated counterparts. While JA treatment exhibited a similar regulatory trend to IAA, the overall quantity of DEGs remained comparatively lower under JA treatment (Figure S11B,C).

The biological processes—including stimulus response, cell communication, and hormone response, among others—were markedly amplified following IAA or JA application, demonstrating pronounced enrichment within their respective regulatory pathways (Figure S12A, B). Meanwhile, various metabolic processes were activated (Figure S12C,D). Most genes were enriched in a similar KEGG pathway, while some DEGs in the JA treatment group were mainly enriched in the MAPK signaling pathway. A large number of genes were regulated in a similar pattern by the exogenous IAA and JA application (Figure S12E–G), and among which the expression levels of sucrose and starch metabolism related genes (Figure S13), auxin-specific genes, and JA biosynthetic pathway genes (Figure S14) were increased in both hormones treated groups. These results suggested that IAA and JA might share the same gene regulatory pathway in the AR primordia establishment. The qRT-PCR outcomes of structural genes (Table S2), were also significantly correlated with RNA-seq (Figure S15A,B).

A total of 65 pathways from 30 specimens obtained via gene set variation analysis (GSVA) were subjected to the co-expression network construction (Figure S16). According to the clustering of genes based on the topological overlap, a total of 18 gene modules were eventually filtered out (Figure S17A). The correlation among the featured genes of each module showed that the bisque4, orangered4, and indianred4 modules had the highest correlation with the KEGG and hormone signaling pathways (Figure S17B). WGCNA analysis was conducted on these three modules separately, and it was found that all three modules contain hub genes with the following IDs:

Unigene0097724 (*CRL1*), Unigene0007991 (*GH3.8*) and Unigene0093342 (*AOS1*) (Figure S17C–E). The expression of all three hub genes was upregulated in root primordium initiation stage and after the exogenous IAA and JA application. Therefore, these three genes were selected for further functional investigations.

Expression pattern analyses and functional study of CRL1, AOS1, and GH3.8

To determine the specific expression of *DbCRL1*, *DbGH3.8*, and *DbAOS1*, RT-qPCR was performed with different parts of *D. brandisii* culm (Figure S18). Based on the distribution of roots, the culm was divided into four sections, including Culm Base I (1st–2nd node), Clum Base II (3rd–4th node), Clum Base III (5th–7th node), Clum Base IV (14th–18th node) (Figure S18A). The number of roots in the nodes decreased gradually with the increment of nodes (Figure S18B). The results of RT-qPCR demonstrated that the expression levels of *DbCRL1* and *DbGH3.8* showed a constantly decreasing trend with culm height, which was completely consistent with the change of root points along the culm, while *DbAOS1* was not detected (Figure S18C). Further *in situ* hybridization (ISH) results (Figure S19) showed that *DbCRL1* and *DbGH3.8* had a similar expression pattern in the cortex, which were located in AR primordia at the differentiation stage (Figure S19D–F). The absence of detected *DbAOS1* indicated that the elevated level of JA was not produced in the branch bases or nodes during AR differentiation, suggesting an alternative tissue origin.

To gain a deeper knowledge of their function, these three genes were overexpressed in rice. The experiments showed that overexpression of *DbAOS1* (L#1) and *DbCRL1* (L#3) could enhance ARs, while overexpression of *DbGH3.8* (L#2) and mutagenesis of *OsCRL1* (L#4) inhibited ARs formation (Figure S20A–G). The results implied that *GH3.8* played a negative role in AR formation. In L#1 and L#3 lines, the number and length of roots were significantly promoted (Figure S20F,G). A descent range of AR number observed in the seedlings of rice under IAA conditions was significantly lower than that of WT, while *DbGH3.8* played a positive role in ARs formation under the higher concentrations of IAA, potentially by balancing IAA levels at the branch bases.

DbCRL1 interacted with DbWOX11 *in vivo* and *in vitro*

Previous results suggested that *CRL1*/*JMJ706* expression can be regulated by *WOX11*, controlling CR development (Geng et al., 2024). In bamboos, *CRL1* and *WOX11* showed high expression in *D. brandisii* but decreased in *F. yunnanensis*, and were not detected in *P. mannii*. Furthermore, *DbCRL1* and *DbWOX11* were slightly upregulated in the branch base treated by IAA or JA. To investigate whether there were interactions between them, yeast two-hybrid (Y2H) was performed. The results showed BD-*DbCRL1* and AD-*DbWOX11* co-transformed experimental group; the positive control exhibited normal growth on the QDO plate and displayed blue colonies with X-α-gal (Figure 6a). Subsequently, bimolecular fluorescence complementation (BiFC) assay and coimmunoprecipitation were employed to analyze the interaction between *DbCRL1* and *DbWOX11*. The pGBKT7-*DbCRL1* and PGADT7-*DbWOX11* vectors were constructed and transformed into *Agrobacterium tumefaciens*, which were injected in tobacco leaves. There was an interaction between *DbCRL1* and *DbWOX11* in tobacco leaves, which was mainly located in the nuclear region, with a small amount of expression in the cytoplasm (Figure 6b). Coimmunoprecipitation assay demonstrated that *DbCRL1* could be immunoprecipitated together with *DbWOX11* in rice cells transfected with Pro35S:*DbCRL1*-MYC and Pro35S:*DbWOX11*-GFP (Figure 6c), indicating that *DbCRL1* associated with *DbWOX11 in vivo*.

DISCUSSION

AR formation could effectively improve the propagation of plants and facilitate their adaptation to the environment. AR formation was also a complex developmental process controlled by a plethora of endogenous and environmental factors, cross-linked hormonal networks, genetic factors, and transcriptional cascades (Lakehal & Bellini, 2019).

Anatomical characteristics of ARs formation in the branch bases of *D. brandisii*

The locations of ARs varied with different plant species. In rice and maize, ARs naturally arise from the compressed nodes at the shoot-root junction (Singh et al., 2023). Hochholdinger et al. (2004) considered that only the root primordia at the non-elongated basal nodes can develop and form ARs. Similarly, there were many root points at the culm bases (from the first node to the fourth node) of *D. brandisii* (Figure S19A), which usually formed in the wet season. The number of root points gradually decreased with culm height, and almost no root points could be observed at or above the eighth node above ground. Meanwhile, the branches of *D. brandisii* could also generate AR naturally at the bases. Generally, ARs were more easily induced from the branch bases in those bamboo species with intensive nodes and low-lignified epidermis and cortex cells. The thick cortex layer and low degree of lignification were beneficial for the root primordium differentiation in the branch bases.

The rooting difficulty of cuttings varied among different bamboo species. The branch bases of *D. brandisii* could generate ARs naturally in the environment with high humidity and temperature in the wet seasons, so they could be cut and used as vegetative propagation materials. However, it typically requires about 1 year to generate ARs for the branches of *F. yunnanensis*, which was mainly

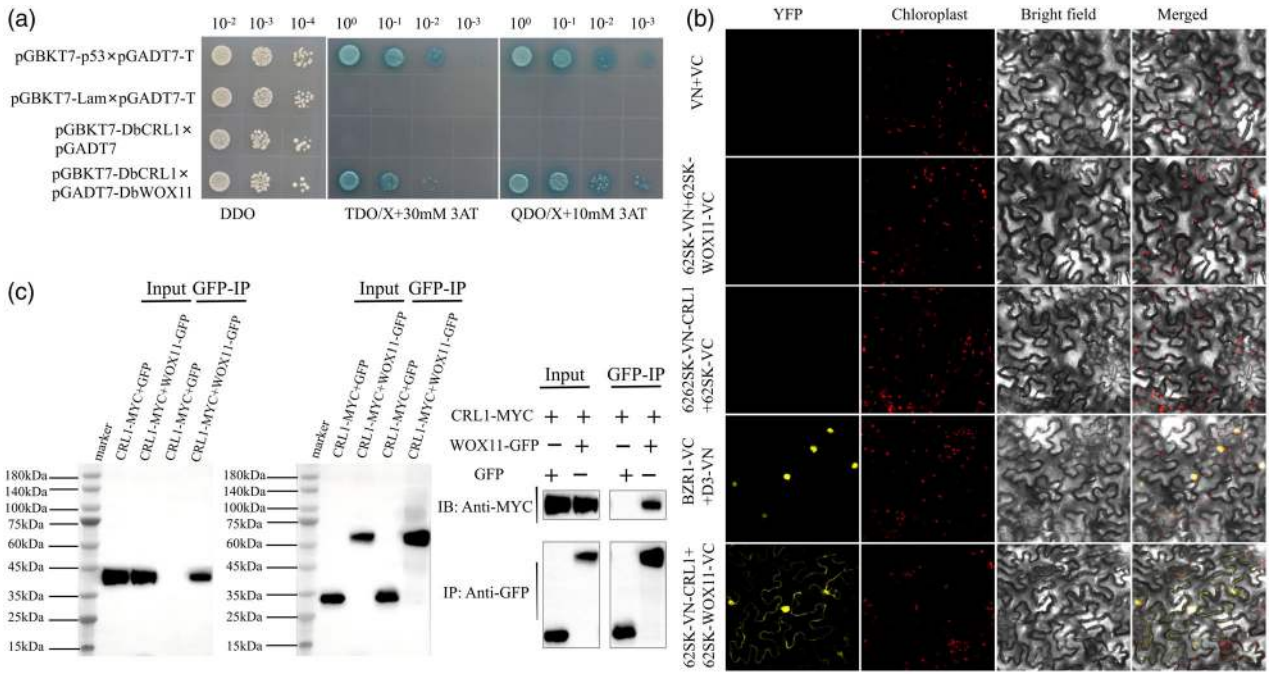

Figure 6. *DbCRL1* interacts with *DbWOX11 in vivo* and *in vitro*.
(a) Detection of *DbCRL1* interaction with *DbWOX11* by yeast two-hybrid assay.
(b) BiFC assay of *DbCRL1* and *DbWOX11*.
(c) Coimmunoprecipitation assay of *DbCRL1* and *DbWOX11 interaction* in rice cells. *CRL1*-MYC construct was transfected with *WOX11*-GFP.

because of their thin cortex layer and high lignification degree. As for *P. mannii*, the branch bases could not generate ARs at all due to their thinner cortex and higher lignification degrees. Unlike *D. brandisii*, the branch bases of *P. mannii* and *F. yunnanensis* lack the compressed internodes. Generally, it could be concluded that the difficulty of rooting was closely related to the anatomical characteristics of branch bases.

Sugar metabolism in AR differentiation

Plants coordinate growth and development with nutrient availability (Fredes et al., 2019; Yoon et al., 2021). In the rooting process of vegetative propagation, the differentiation and development of root primordia require a large amount of nutrients (Giehl et al., 2012). Starch and soluble sugar play a crucial role in AR differentiation (Steffens & Rasmussen, 2016). Compared with stage I of AR differentiation in *D. brandisii*, the starch content decreased and the content of soluble sugar, especially D-glucose and UDP glucose, increased. Correspondingly, the enzyme activities and DEGs related to sugar metabolism also changed, which demonstrated that the starch was decomposed and converted into soluble sugars, providing necessary nutrients for AR initiation. It had also been reported that sucrose and IAA cooperatively regulated AR formation in lotus (Cheng et al., 2020). Sucrose affected AR formation by improving IAA content at the induction stage, and increased sucrose content might also be required for AR development (Cheng et al., 2020). Similarly, the present study also demonstrated that the exogenous IAA and JA increased the soluble sugar contents and activities of related enzymes in the branch bases of *D. brandisii*, which provided nutritional support for the division and differentiation of root primordial cells.

On the contrary, the activities of enzymes related to starch synthesis decreased during branch rooting of *D. brandisii*, such as SSS, GBSS, and AGP, which was possibly due to the consumption of mass carbohydrates and energy for AR initiation and development. Sucrose is degraded into glucose and fructose by *INV*, which regulates internode elongation by regulating the cell osmotic pressure (Guo et al., 2020). It is also involved in various growth and developmental processes including cell division, seed germination, and floral induction, etc. (Yoon et al., 2021). During AR primordia initiation and formation in *D. brandisii* branches, the genes regulating sucrose synthesis were downregulated, while those involved in sucrose degradation were all upregulated, such as *INV* and *SUSY*. This indicated that sucrose was constantly degraded for the energy consumption during the process of branch rooting.

Key hormones in AR differentiation

Phytohormones play important roles as regulators of constitutive and inducible AR formation. Auxin is the major

growth-promoting factor for AR initiation (Gonin et al., 2019). A higher concentration of auxin is required for AR formation during the early steps than during the later steps (Roychoudhry & Kepinski, 2022). Similarly, the concentration of endogenous IAA in the branch bases increased significantly from stage I to stage II, and then decreased sharply, which indicated that a high concentration of IAA was essential for the initiation of root primordium. In *D. brandisii*, the application of exogenous IAA significantly increased the endogenous IAA content in the branch bases, suggesting that exogenous auxin may play a role in rooting by enhancing the level of endogenous IAA. This accumulation of IAA then induced the differentiation of parenchyma cells into AR primordia.

JA is usually reported to play a role in defense response (Pieterse et al., 2012; Yang et al., 2012), abiotic stress (Yan et al., 2018), reproductive development, and tissue regeneration (Ikeuchi et al., 2017; Zhou et al., 2019). Currently, few studies focused on the relationship between JA and root differentiation, and most works considered that JA inhibits ARs initiation and root development (Dob et al., 2021). Alsoufi et al. (2019) and Rogowska et al. (2022) also reported that hairy root biomass was significantly reduced after incubation with JA, due to a lack of secondary growth and an increased cell wall lignification. Other works reported that auxin promotes ARs differentiation by modulating homeostasis of the negative regulator JA in Arabidopsis (Gutierrez et al., 2012). However, a study from Zhu et al. (2006) presented that the application of JA could interact with ethylene and promote the growth of root hair in Arabidopsis. Exogenous JA induced an increase in CR number of rice in a concentration-dependent manner (0.5–12.5 μM) by regulating *OsGER4* (To et al., 2022). Recently, Wan et al. (2025) considered that successive application of JA enhanced root regeneration from Arabidopsis cuttings under 200 mM mannitol condition. In this study, we noticed that different concentrations of JA showed different effects on the ARs differentiation of *D. brandisii*. The application of low JA concentration could promote the ARs differentiation, while the high JA concentration inhibited this process. Compared to the IAA treatment, the exogenous JA treatment apparently increased the number and diameter of ARs but was shorter in length, which implied that the roles of JA were not completely the same as those of IAA in root induction.

Expression patterns of key genes related to ARs differentiation in the branch bases of *D. brandisii*

There are not many genes related to AR differentiation that have been identified. The first AR-related gene discovered in rice was ADVENTITIUS ROOTLESS1/CROWN ROOTLESS1 (*ARL1*/*CRL1*), and the absence of *ARL1*/*CRL* leads to the deficiency of ARs in rice (Inukai et al., 2005; Liu et al., 2005). *CRL1* functions synergistically with *WOX11* to enhance rice CR development (Geng et al., 2023). In this study, *DbCRL1* was verified to effectively promote the rooting number of rice seedlings, indicating that *DbCRL1* played an essential role in controlling AR differentiation in bamboo. The functional relationship between *DbCRL1* and *DbWOX11* demonstrated that *DbWOX11* enhanced *DbCRL1* to promote AR initiation and growth. WOX11 also activates CKX4 expression to reduce cytokinin levels at root emergence and elongation stages (Geng et al., 2023). Our results showed the content of tZ significantly decreased at the ARs differentiation stage and the application of exogenous IAA or JA; thus, the DbCRL1-DbWOX11 module might be required in maintaining cytokinin homeostasis. The hot and humid weather conditions induced the endogenous IAA and JA synthesis by increasing the expressions of *YUCCA* and *AOS1*, then activated the expression of *CRL1*, which further initiated the AR differentiation. Additionally, the accumulated IAA and JA mutually facilitated their synthesis in the branch bases, which further increased the AR differentiation.

GH3s usually catalyze the binding of IAA and JA with amino acids, thereby reducing the level of free IAA and controlling JA homeostasis (Gutierrez et al., 2012). The enzymes GH3.3, GH3.5, and GH3.6 redundantly promote ARI by conjugating JA to amino acids (Gutierrez et al., 2012). Ding et al. (2008) considered that *GH3.8* might activate a JA signaling-independent pathway. The spatial expressions of *GH3.8* were entirely consistent with the roots distribution in *D. brandisii*, with higher expressions detected in the culm and branch bases. We also confirmed that the overexpression of *GH3.8* inhibited the AR differentiation of rice seedlings inoculated in the medium with low IAA content, but a large number of ARs were formed when cultivated in the medium with high IAA content. In the present study, it was noticed that *GH3.8* was upregulated in the *D. brandisii* branch bases no matter under the exogenous IAA application or under the exogenous JA treatment, implying this gene played an important regulatory role to balance the concentrations of IAA and JA in the branch bases.

Dob et al. (2021) found that *MYC2-dependent* JA signaling inhibits AR formation by downregulating the expression of the cytokinin oxidase/dehydrogenase 1 gene. Nevertheless, *MYC2 was* upregulated during AR differentiation in *D. brandisii*, demonstrating that *MYC2* might increase the expression of JA-related genes and enhance the synthesis of JA. Chen et al. (2011) consider that JA inhibits root growth by interacting with auxin, and exogenous JA treatment inhibits the expression of auxin-responsive transcription factors *PLETHORAs* (*PLTs*), thereby damaging the stem cell niche and cell proliferation. However, it was reported that JA-responsive *MYC2* is required for root regeneration and growth by inhibiting

wound-promoted auxin production (Mähönen et al., 2014; Wan et al., 2025). In our research, the content of JA and its precursor substances continued to increase until AR formation. The number of JA-related genes changed accordingly. The *AOS1* expression level increased during AR differentiation, and the overexpression of *AOS1* promoted root growth, which was consumed with the fact that the exogenous JA application could promote AR differentiation at the branch base. This implied that the low concentration of JA might initiate AR differentiation via another signal pathway that has yet to be identified.

Interaction of IAA and JA during ARs differentiation

The interaction between JA and auxin plays a role in plant development and physiological processes such as cell elongation and production of secondary metabolites (Saniewski et al., 2002). Paradoxically, some works reported that the root elongation of wheat was inhibited by increasing the endogenous IAA and JA levels in roots via upregulating the key gene expressions related to IAA biosynthesis/transport (*TDC*, *YUC1*, and *PIN9*) and JA metabolism (*LOX8*, *AOS1*, *AOC1*, and *JAR1*) (Nguyen et al., 2018).

It was fascinating to observe that exogenous application of IAA not only propelled an elevation in the endogenous IAA content but also enhanced the endogenous JA content in the branch bases (Figure S10K,M). The application of exogenous JA also raised the endogenous IAA content (Figure S10K), suggesting a mutually enhancing role for IAA and JA in synthesis. Nevertheless, the exogenous JA did not boost the endogenous JA content in the branch base, suggesting that the application of exogenous JA could also promote AR differentiation by enhancing the endogenous IAA synthesis. In our research, *ASA1* was significantly upregulated no matter during AR differentiation stages or under the JA treatment. This gene enhanced the synthesis of auxin precursors (tryptophan), suggesting that JA might interact with auxin through a tryptophan-dependent auxin synthesis pathway. Similarly, the exogenous IAA also increased the expression of *AOS1*, and then increased the JA contents in the branch bases during AR differentiation. Interestingly, the exogenous application of JA and IAA at low concentrations could enhance the expression of *CRL1* and *WOX11*. DbCRL1 could directly promote rooting, and it also interacted with DbWOX11 to activate the initiation of root primordia. These results suggested JA could not only directly enhance AR initiation, but also might promote AR formation via 'JA-ASA1-IAA' pathway. Additionally, JA might trigger AR differentiation through a distinct signaling pathway from that of IAA, resulting in a notable difference in the morphological features of roots compared to those induced by IAA. Therefore, we established the regulation pattern of IAA and JA in AR differentiation in the branch base of *D. brandisii* (Figure 7) according to the results.

MATERIALS AND METHODS

Plant materials

All samples of three types of bamboo species were cultivated in the bamboo garden of Southwest Forestry University (E 102°10′~103°40′, N 24°23′~26°22′). When the main branches of 1-year-old *D. brandisii* culms reached up to 15–20 cm (about 1 month after budding from node part of culm), ARs differentiated and developed in the following week, which included four stages: root undifferentiation (Stage I: at 0 day), root primordia initiation (Stage II: at second day), root primordia formation (Stage III: at third day), and root formation (Stage IV: at seventh day). The branch bases were separately sampled at the different four stages for histological, physiological, and molecular determination in May 2020, which was the local rainy season. Two other types of bamboo species (difficult-to-root in the branch base), that is, *F. yunnanensis* and *P. mannii* at the same developmental degrees were selected to compare the anatomical differences in the branch base. This is because the AR induction was difficult in the branch base of *F. yunnanensis* and more difficult in the branch base of *P. mannii*. Moreover, no successful cutting propagation was reported in the branch of *Phyllostachys* bamboos so far.

Anatomical characteristic of branch base in different types of bamboos

The samples of all stages among the different types of bamboo were chosen for anatomical feature analysis. Each sample was repeated three times. For young materials, 36 samples from bamboo branch bases were cut off and fixed in Formalin-Aceto-Alcohol solution (90% alcohol + 5% acetic acid + 5% formaldehyde) for vacuum fixation treatment. The materials were dehydrated sequentially by using a mixture of alcohol and tert-butanol from low to high levels, and then waxed and sliced with a thickness of 7 μm by Leica RM2165 (Leica Inc., Wetzlar, Germany). For harder materials such as *F. yunnanensis* and *P. mannii*, 12 samples from the branch bases were cut off and soaked in an ethanol glycerol (1:1) softener for vacuum fixation treatment, and then the materials were embedded in a melted polyethylene glycol liquid. The sections were sliced in both horizontal and vertical directions with a thickness of 20–25 μm by using LEICA SM2010R (Leica Inc.), and then were dewaxed with xylene, rehydrated in graded alcohol, and stained with Saffranine O and fast green. Afterwards, they were redehydrated in graded alcohol. After being transparent with xylene, they were sealed with neutral gum and photographed under an optical microscope. The relationship between the base structure of different bamboo branches and the difficulty of rooting was analyzed through photography observation.

Determination of carbohydrate metabolism and hormone contents in branch bases during ARs differentiation in *D. brandisii* branches

The endogenous starch and soluble sugar contents in the bases of young branches at all stages were measured according to the method of Wang et al. (2020). The determination of glucose, fructose, and sucrose content was carried out referring to the method of Georgelis et al. (2018). The cellulose content in the base of the young branch was measured according to the methods of Yu et al. (2021). The identification and quantification of plant hormones were accomplished by Wuhan MetWare Biotechnology Co. Ltd. (Wuhan, China) based on the AB Sciex QTRAP 6500 LC-MS/MS platform. Samples were treated according to Luo et al. (2021).

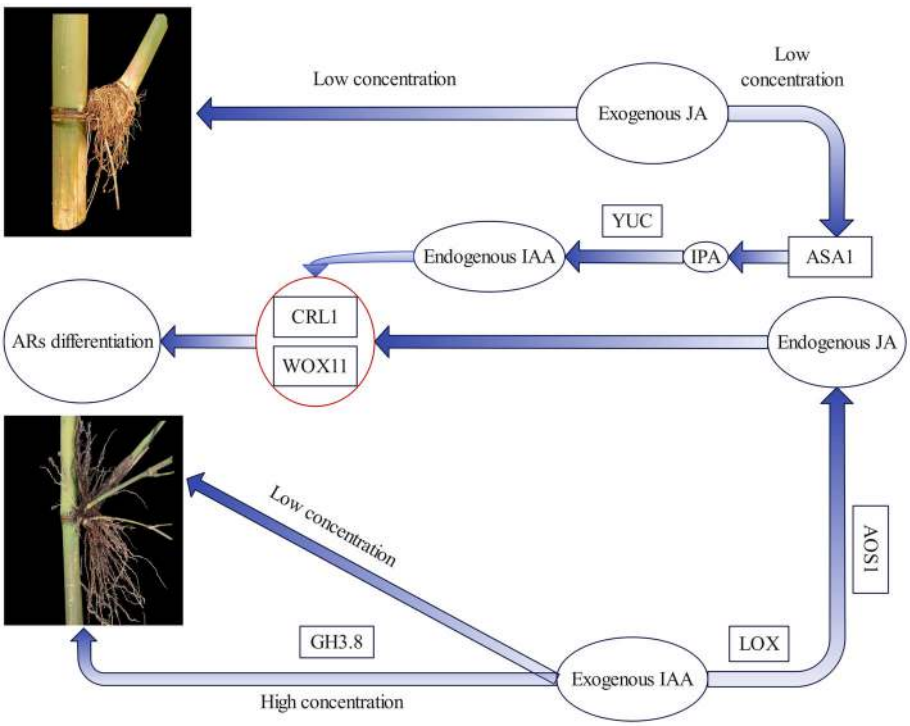

Figure 7. Integration of multi-osmic regulatory networks of exogenous hormones on adventitious root differentiation of *Dendrocalamus brandisii*. Low concentration of IAA and JA. The metabolites (oval box) can affect the biosynthesis of hormone (hexagon box), which processes are regulated by genes (Re).

The extraction of crude enzymes was conducted according to the methods of Yu et al. (2021). Activity determination of starch metabolizing enzymes, including SSS, GBSS, STP and AGP, followed the methods outlined by Wang et al. (2020). VIN activity was determined according to Weiszmann et al. (2018). SAI, insoluble extracellular invertase (CWI) and SUSY were assessed as described by Wang et al. (2020).

Determination of metabolites in *D. brandisii* branch bases during ARs differentiation

The detection and identification of metabolites were conducted according to Chen et al. (2013). Significant upregulations of metabolites between groups were identified with both VIP and absolute values of Log2FC (fold change) ≥1. Pathways with significantly regulated metabolites were mapped to metabolite sets enrichment analysis, with their statistical significance assessed using *P*-values from hypergeometric tests.

RNA sequencing and data analysis of branch bases in different bamboo species under natural conditions

The young and mature branch bases of *D. brandisii*, *F. yunnanensis*, and *P. mannii* were sampled to analyze the gene expression difference in root differentiation between bamboo species. RNA sequencing libraries of each sample were constructed and sequenced by Wuhan MetWare Biotechnology Co. Ltd. as described previously (Chen et al., 2019). DEGs were identified using Cuffdiff, and a list of genes with at least two fold change (log2 fold change ≥1) and FDR correction <0.05 was considered as screening conditions. Gene ontology was performed using the BiNGO plug-in of Cytoscape (version 3.7.1) with *P*-value ≤0.05.

Quantitative real-time PCR (qRT-PCR) was carried out using gene-specific primers (Table S1) to validate the transcriptome data according to Zhao et al. (2020).

Correlation analysis between DEGs and differential metabolites during ARs differentiation in *D. brandisii* branches

Correlations between DEGs and differential metabolites were conducted with the Pearson correlation coefficient (CC) ($R > 0.8$) during AR differentiation. The expression levels of the filtered DEGs and metabolites were shown in the histogram at stage I/II and stage III/IV, respectively. Based on KEGG annotation of the transcriptome, combined with the correlation analysis diagram of hormones, corresponding feature modules were established. Hormones were analyzed by expression heatmaps, hierarchical clustering, and selecting stable hormones with higher levels. The HeatMap package of TBtools was applied to visualize the data of the hormone difference matrix according to the OTU results.

Effects of IAA and JA on cutting propagation and tissue culture plantlet of *D. brandisii*

The cutting propagation was performed using the mature and hardened culms with six nodes from 2-year-old culms in April. Selected culms with branches were embedded in a matrix of red soil and humus soil (1:1) and then treated with aqueous solutions of varying concentrations of IAA (ranging from 0 to 200 mg L^{-1}), alongside JA to assess their impact on AR development. Each treatment comprised 30 branches across three replicates, with the aqueous solution applied every 10 days. The length and diameter

of ARs were precisely measured using a standard ruler and digital vernier caliper, and the number of roots was also recorded across various treatment groups following a 40-day period.

Building upon the cutting results and previous investigations (Fattorini et al., 2018), the unrooted *D. brandisii* plantlets were systematically cultivated in MS medium supplemented with 0, 10, 20, and 30 μM concentrations of IAA and JA for AR differentiation. Each treatment group comprised 20 plantlets, with the entire experimental setup replicated three times for statistical rigor. The morphological characteristics of roots were examined under various hormone concentrations after 30 days of treatment.

Physiological and transcriptomic changes in *D. brandisii* branch bases after being treated with IAA and JA

To verify whether IAA and JA play a crucial role in AR differentiation of the branch bases, a total of 150 1-year-old *D. brandisii* culms under the same growth status were selected, and the branches were sampled at 0, 12, 24, and 36 h after the exogenous IAA and JA (10 μM, mixed with lanolin) application in April. The changes in sugar metabolism, endogenous hormones contents, DEGs, and their relationships were analyzed in the sampled branches. The identification and quantification of plant hormones were accomplished, and the RNA sequencing libraries of each sample were constructed and sequenced by Gene Denovo Biotechnology Co. Ltd (Guangzhou, China). The data analysis and validation were the same as previous. The sequence of genes selected for validation was shown as Table S2.

Network construction between gene expression and hormones and identification of hub genes

The GSVA package in R software was used for the potential changes in pathway activity in each sample. The gene sets were screened and filtered according to Hänzelmann et al. (2013). The 'WGCNA' R package was used to screen for ARs-related pathways and genes in the dataset obtained from GSVA according to Wang et al. (2023). The Pearson CC was used to determine the association between each module and characteristics. The CC was greater than 0.7, and the data selection threshold was 9. Genes obtained from WGCNA and DEGs between the branch base treated with hormone and controls were entered into a search tool on STRING to identify hub genes. Cytoscape (v. 3.7.1) was used to visualize the networks.

ISH of hub genes in branch base and relative expression analysis of genes related to ARs initiation in *D. brandisii* culms

The samples from the branch bases during ARs initiation were cut off and fixed in paraformaldehyde fixative, dehydrated through an ethanol series, and embedded in paraffin (Chu et al., 2020). About 4 μm-thick cross sections were cut using the microtome (Leica Inc.). The sections were placed on the poly-L-lysine coated glass slides. For preparing DIG-UTP-labeled riboprobes, a 535 bp gene-specific region of *DbCRL1*, 936 bp of *DbAOS1*, and 836 bp of *DbGH3.8* were cloned into *p*Bluescript SK^+ as a blunt insert in the *Eco*RV site. The anti-sense probe for all genes hybridized to the target transcript was detected by anti-DIG antibodies. Hybridization was performed on cross sections as described by Houben et al. (2006). The sections were mounted in Entellan and photographed under the microscope.

The 1-year-old bamboo culm was selected to observe the bulges in September. To detect the relative expression of genes related to AR initiation in different parts of *D. brandisii* culm, qRT-PCR was performed according to the methods described above.

Functional verification of key genes related to root differentiation via transgenic technology

Full length mRNA-Seq was derived from the young branch base of *D. brandisii* (PRJNA890860) (Gene Denovo Biotechnology Co. Ltd, Guangzhou, China). For generating ectopic overexpression construction, *DbAOS1*, *DbCRL1*, and *DbGH3.8* were cloned in *p*BWA(V) HS, respectively. Meanwhile, pYLCRISPR/Cas9 Pubi-H-osu3 was constructed for evaluating *CRL1* with the CRISPR-Cas9 system using primers t1–t2(+) and t1–t2(−). The primer sequences were shown in Table S3. The functions of the three genes were verified by employing the transgenic technology in rice according to the previous methods reported by Chen et al. (2015) and Mao et al. (2020). The construction of recombinant plasmid and rice transformation were performed by Wuhan Biorun biological company. The T0 transgenic rice plants were grown to 7 days for AR phenotype after being inoculated into the rooting medium. For IAA treatment, the wild-type and *DbGH3.8* overexpression lines were grown on MS media supplemented with 300 μM of IAA (Sigma, St. Louis, MO, USA). AR phenotype and qRT-PCR were all performed according to methods described above. Control plants were generated from rice transformation using empty pBWA(V)HS without the cloned gene following the same procedures.

Interactive verification of DbCRL1 and DbWOX11

For Y2H assay, the ORF sequence of *DbCRL1* was ligated into the GAL4 binding domain vector (pGADT7), and the ORF sequence of *DbWOX11* was ligated into the GAL4 activation domain vector (pGBKT7). Two constructs were co-transformed into yeast strain AH109. The transformants were filtered by the selected dropout medium SD/-Trp/-Leu/-His/-Ade (QDO) or QDO +X-α-gal for 5 days to assess their growth status.

For the BiFC assay, the ORFs of *DbCRL1* and *DbWOX11* were cloned and inserted into pGBKT7-ccdb and pGreenII-62-SK-VC173 vectors to construct pGBKT7-*DbCRL1* and PGADT7-*DbWOX11*, respectively. The positive construct was transformed into *A. tumefaciens* strain GV3101. The combination was then infiltrated into tobacco leaves for fluorescence observation by using confocal microscopy. The yellow fluorescence protein signal was obtained with a 511 nm wavelength, collecting emission with a 525 nm bandpass filter. Meanwhile, tobacco leaves infiltrated for 3 days were assayed for co-immunoprecipitation. The leaves were ground in liquid nitrogen and resuspended with IP Lysis buffer, and then centrifuged at 4°C; anti-MYC was added and incubated for 1 h at 25°C. Immunoprecipitates were analyzed by Western blot (Yang et al., 2024).

Statistical analysis

Randomized block design was used for the experiment with three replicates per treatment for bamboos and 15 replicates per treatment for rice. Each experiment was repeated thrice. All data were presented as mean ± SD. Significant differences between two groups were determined with the Tukey–Kramer post-test or Dunnett's T3 method. The data were subjected to analysis of variance and Duncan Multiple Range Test at 5% significance by SPSS ver. 17 (SPSS Inc., Armonk, NY, USA). Correlation among hub DEGs and metabolites was evaluated using Pearson's correlation analysis.

AUTHOR CONTRIBUTIONS

LY, DJ, CC, and LL analyzed the experimental data and completed most of the experiments. HZ, JL, and CW collected and processed the samples. SW designed the experiment; LY, TFS, and SW wrote the manuscript. All authors read and approved the final manuscript.

CONFLICT OF INTEREST

No conflicts of interest declared.

ACKNOWLEDGEMENTS

This paper was funded by the National Key R and D Program of China (2021YFD2200503), the Natural Science Foundation of Yunnan Province (202201AS070018), and the National Natural Science Fund of China (32460376). The authors thank the Key Laboratory of Forest Biotechnology in Yunnan Province (College of Biological Science and Food Engineering, Southwest Forestry University), Wuhan MetWare Biotechnology Co. Ltd., and Gene Denovo Biotechnology Co. Ltd (Guangzhou, China) for the LC–MS/MS analysis and RNA sequencing.

DATA AVAILABILITY STATEMENT

The sequence data have been deposited in the National Center for Biotechnology Information Short Reads Archive (PRJNA890860, PRJNA896250, PRJNA897021, PRJNA 895226, and PRJNA898091), and are also available from the corresponding author upon reasonable request.

SUPPORTING INFORMATION

Additional Supporting Information may be found in the online version of this article.

Dataset S1. Normalized read counts of *Dendrocalamus brandisii* genes: sample description.

Dataset S2. Normalized expression data of *Fargesia yunnanensis* genes.

Dataset S3. Normalized expression data of *Phyllostachys mannii* genes.

Dataset S4. Normalized expression data of *Dendrocalamus brandisii* genes.

Table S1. A list of genes selected for validation of their regulation in different developmental stages.

Table S2. A list of genes selected for validation of their regulation upon the exogenous IAA and JA treatment.

Table S3. Primer information of genes for genetic transformation.

Figure S1. Dynamical changes of sugar metabolism of the branch base during ARs differentiation in *Dendrocalamus brandisii*.

Figure S2. Dynamical changes of endogenous hormone content of the branch base during ARs differentiation in *Dendrocalamus brandisii*.

Figure S3. Differential metabolites and KEGG categorization in *Dendrocalamus brandisii* at stage I/II, II/III, III/IV, respectively.

Figure S4. GO enrichment of *Fargesia yunnanensis* and *Phyllostachys mannii* in the branch base.

Figure S5. GO enrichment and heatmap of *Dendrocalamus brandisii* in the branch base during AR differentiation.

Figure S6. Validation of genes for qPCR analysis of *Dendrocalamus brandisii* during AR differentiation.

Figure S7. Pearson correlation analysis between gene expression and metabolite accumulation.

Figure S8. Effects of exogenous IAA and JA on adventitious root formation of the cuttage seedlings.

Figure S9. Effects of exogenous IAA and JA on adventitious root formation of tissue culture seedlings.

Figure S10. Dynamical changes of soluble sugar, starch, the related enzymes and endogenous hormones of the branch base treated with IAA and JA in *Dendrocalamus brandisii*.

Figure S11. Time influence on *Dendrocalamus brandisii* transcriptome response to IAA and JA.

Figure S12. GO enrichment and KEGG pathway of *Dendrocalamus brandisii* treated by IAA and JA.

Figure S13. Changes in sugar metabolism pathway-related genes after external application of IAA and JA at the base of branches in *Dendrocalamus brandisii*.

Figure S14. Changes in hormone signaling pathway-related genes after external application of IAA and JA at the base of branches in *Dendrocalamus brandisii*.

Figure S15. Fold change of RNAseq and relative expression of *Dendrocalamus brandisii* by qRT-PCR treated by IAA and JA.

Figure S16. Clustering of module eigengenes from specimens treated by IAA and JA.

Figure S17. Characterization of hub genes and mRNA-hormone network construction.

Figure S18. Relative expression of ARs formation genes in the culms of *Dendrocalamus brandisii*.

Figure S19. *In situ* hybridizations of *Dendrocalamus brandisii* cortex with key gene-specific probes.

Figure S20. Function of key genes in transgenic rice.

REFERENCES

Alsoufi, A., **Pączkowski, C.**, **Szakiel, A.** & **Długosz, M.** (2019) Effect of jasmonic acid and chitosan on triterpenoid production in *Calendula officinalis* hairy root cultures. *Phytochemistry Letters*, **31**, 5–11. Available from: https://doi.org/10.1016/j.phytol.2019.02.030

Atkinson, J.A., **Rasmussen, A.**, **Traini, R.**, **Voß, U.**, **Sturrock, C.**, **Mooney, S.J.** ***et al.*** (2014) Branching out in roots: uncovering form, function, and regulation. *Plant Physiology*, **166**, 538–550. Available from: https://doi.org/10.1104/pp.114.245423

Bellini, C., **Pacurar, D.** & **Perrone, I.** (2014) Adventitious roots and lateral roots: similarities and differences. *Annual Review of Plant Biology*, **65**, 639–666. Available from: https://doi.org/10.1146/annurev-arplant-050213-035645

Chaturvedi, K., **Singhwane, A.**, **Dhangar, M.**, **Mili, M.**, **Gorhae, N.**, **Naik, A.** ***et al.*** (2023) Bamboo for producing charcoal and biochar for versatile applications. *Biomass Conversion and Biorefinery*, **14**, 1–27. Available from: https://doi.org/10.1007/s13399-022-03715-3

Chen, L., **Wu, Q.**, **He, W.**, **He, T.**, **Wu, Q.** & **Miao, Y.** (2019) Combined *de novo* transcriptome and metabolome analysis of common bean response to *Fusarium oxysporum* f. sp. *phaseoli* infection. *International Journal of Molecular Sciences*, **20**(24), 6278. Available from: https://doi.org/10.3390/ijms20246278

Chen, Q., **Sun, J.**, **Zhai, Q.**, **Zhou, W.**, **Qi, L.**, **Xu, L.** ***et al.*** (2011) The basic helix-loop-helix transcription factor MYC2 directly represses PLETHORA expression during jasmonate-mediated modulation of the root stem cell niche in Arabidopsis. *The Plant Cell*, **23**(9), 3335–3352. Available from: https://doi.org/10.1105/tpc.111.089870

Chen, W., **Gong, L.**, **Guo, Z.**, **Wang, W.**, **Zhang, H.**, **Liu, X.** ***et al.*** (2013) A novel integrated method for large-scale detection, identification, and quantification of widely targeted metabolites: application in the study of rice metabolomics. *Molecular Plant*, **6**(6), 1769–1780. Available from: https://doi.org/10.1093/mp/sst080

Chen, X., **Lu, S.**, **Wang, Y.**, **Zhang, X.**, **Lv, B.**, **Luo, L.** ***et al.*** (2015) OsNAC2 encoding a NAC transcription factor that affects plant height through

mediating the gibberellic acid pathway in rice. *The Plant Journal*, **82**(2), 302–314. Available from: https://doi.org/10.1111/tpj.12819

Cheng, L., **Zhao, M.**, **Hu, Z.**, **Liu, H.** & **Li, S.** (2020) Comparative transcriptome analysis revealed the cooperative regulation of sucrose and IAA on adventitious root formation in lotus (*Nelumbo nucifera* Gaertn). *BMC Genomics*, **21**(1), 653. Available from: https://doi.org/10.1186/s12864-020-07046-3

Chu, C., **Huang, L.** & **Wang, S.** (2020) Comparison on the anatomical structures of the roots generated from different parts of *Dendrocalamus brandisii*. *Acta Botanica Boreali-Occidentalia Sinica*, **40**(1), 49–58. (in Chinese). https://doi.org/10.7606/j.issn.1000-4025.2020.01.0043

Ding, X., **Cao, Y.**, **Huang, L.**, **Zhao, J.**, **Xu, C.**, **Li, X.** ***et al.*** (2008) Activation of the indole-3-acetic acid-amido synthetase GH3-8 suppresses expansin expression and promotes salicylate- and jasmonate-independent basal immunity in rice. *The Plant Cell*, **20**(1), 228–240. Available from: https://doi.org/10.1105/tpc.107.055657

Dob, A., **Lakehal, A.**, **Novak, O.** & **Bellini, C.** (2021) Jasmonate inhibits adventitious root initiation through repression of CKX1 and activation of RAP2.6L transcription factor in Arabidopsis. *Journal of Experimental Botany*, **72**(20), 7107–7118. Available from: https://doi.org/10.1093/jxb/erab358

Efroni, I., **Mello, A.**, **Nawy, T.**, **Ip, P.L.**, **Rahni, R.**, **DelRose, N.** ***et al.*** (2016) Root regeneration triggers an embryo-like sequence guided by hormonal interactions. *Cell*, **165**(7), 1721–1733. Available from: https://doi.org/10.1016/j.cell.2016.04.046

Fattorini, L., **Hause, B.**, **Gutierrez, L.**, **Veloccia, A.**, **Della Rovere, F.**, **Piacentini, D.** ***et al.*** (2018) Jasmonate promotes auxin-induced adventitious rooting in dark-grown *Arabidopsis thaliana* seedlings and stem thin cell layers by a cross-talk with ethylene signalling and a modulation of xylogenesis. *BMC Plant Biology*, **18**(1), 182. Available from: https://doi.org/10.1186/s12870-018-1392-4

Fredes, I., **Moreno, S.**, **Díaz, F.P.** & **Gutiérrez, R.A.** (2019) Nitrate signaling and the control of Arabidopsis growth and development. *Current Opinion in Plant Biology*, **47**, 112–118. Available from: https://doi.org/10.1016/j.pbi.2018.10.004

Geng, L., **Li, Q.**, **Jiao, L.**, **Xiang, Y.**, **Deng, Q.**, **Zhou, D.X.** ***et al.*** (2023) WOX11 and CRL1 act synergistically to promote crown root development by maintaining cytokinin homeostasis in rice. *The New Phytologist*, **237**(1), 204–216. Available from: https://doi.org/10.1111/nph.18522

Geng, L., **Tan, M.**, **Deng, Q.**, **Wang, Y.**, **Zhang, T.**, **Hu, X.** ***et al.*** (2024) Transcription factors WOX11 and LBD16 function with histone demethylase JMJ706 to control crown root development in rice. *The Plant Cell*, **36**(5), 1777–1790. Available from: https://doi.org/10.1093/plcell/koad318

Georgelis, N., **Fencil, K.** & **Richael, C.M.** (2018) Validation of a rapid and sensitive HPLC/MS method for measuring sucrose, fructose and glucose in plant tissues. *Food Chemistry*, **262**, 191–198. Available from: https://doi.org/10.1016/j.foodchem.2018.04.051

Giehl, R.F., **Lima, J.E.** & **von Wirén, N.** (2012) Localized iron supply triggers lateral root elongation in Arabidopsis by altering the AUX1-mediated auxin distribution. *The Plant Cell*, **24**(1), 33–49. Available from: https://doi.org/10.1105/tpc.111.092973

Gonin, M., **Bergougnoux, V.**, **Nguyen, T.D.**, **Gantet, P.** & **Champion, A.** (2019) What makes adventitious roots? *Plants (Basel)*, **8**(7), 240. Available from: https://doi.org/10.3390/plants8070240

Grewal, R.K., **Saraf, S.**, **Deb, A.** & **Kundu, S.** (2018) Differentially expressed microRNAs link cellular physiology to phenotypic changes in rice under stress conditions. *Plant and Cell Physiology*, **59**(10), 2143–2154. Available from: https://doi.org/10.1093/pcp/pcy136

Guo, X., **Chen, H.**, **Liu, Y.**, **Chen, W.**, **Ying, Y.**, **Han, J.** ***et al.*** (2020) The acid invertase gene family is involved in internode elongation in *Phyllostachys heterocycla* cv. *pubescens*. *Tree Physiology*, **40**(9), 1217–1231. Available from: https://doi.org/10.1093/treephys/tpaa053

Gutierrez, L., **Mongelard, G.**, **Floková, K.**, **Pcurar, D.I.**, **Novák, O.**, **Staswick, P.** ***et al.*** (2012) Auxin controls Arabidopsis adventitious root initiation by regulating jasmonic acid homeostasis. *The Plant Cell*, **24**(6), 2515–2527. Available from: https://doi.org/10.1105/tpc.112.099119

Hänzelmann, S., **Castelo, R.** & **Guinney, J.** (2013) GSVA: gene set variation analysis for microarray and RNA-seq data. *BMC Bioinformatics*, **14**, 7. Available from: https://doi.org/10.1186/1471-2105-14-7

Hochholdinger, F., **Park, W.J.**, **Sauer, M.** & **Woll, K.** (2004) From weeds to crops: genetic analysis of root development in cereals. *Trends in Plant Science*, **9**(1), 42–48. Available from: https://doi.org/10.1016/j.tplants.2003.11.003

Houben, A., **Orford, S.J.** & **Timmis, J.N.** (2006) *In situ* hybridization to plant tissues and chromosomes. *Methods in Molecular Biology*, **326**, 203–218. Available from: https://doi.org/10.1385/1-59745-007-3:203

Ikeuchi, M., **Iwase, A.**, **Rymen, B.**, **Lambolez, A.**, **Kojima, M.**, **Takebayashi, Y.** ***et al.*** (2017) Wounding triggers callus formation via dynamic hormonal and transcriptional changes. *Plant Physiology*, **175**(3), 1158–1174. Available from: https://doi.org/10.1104/pp.17.01035

Inukai, Y., **Sakamoto, T.**, **Ueguchi-Tanaka, M.**, **Shibata, Y.**, **Gomi, K.**, **Umemura, I.** ***et al.*** (2005) Crown root-less1, which is essential for crown root formation in rice, is a target of an auxin response factor in auxin signaling. *The Plant Cell*, **17**(5), 1387–1396. Available from: https://doi.org/10.1105/tpc.105.030981

Jing, T., **Ardiansyah, R.**, **Xu, Q.**, **Xing, Q.** & **Müller-Xing, R.** (2020) Reprogramming of cell fate during root regeneration by transcriptional and epigenetic networks. *Frontiers in Plant Science*, **11**, 317. Available from: https://doi.org/10.3389/fpls.2020.00317

Joshi, M. & **Ginzberg, I.** (2021) Adventitious root formation in crops-potato as an example. *Physiologia Plantarum*, **172**(1), 124–133. Available from: https://doi.org/10.1111/ppl.13305

Lakehal, A. & **Bellini, C.** (2019) Control of adventitious root formation: insights into synergistic and antagonistic hormonal interactions. *Physiologia Plantarum*, **165**(1), 90–100. Available from: https://doi.org/10.1111/ppl.12823

Liu, H., **Wang, S.**, **Yu, X.**, **Yu, J.**, **He, X.**, **Zhang, S.** ***et al.*** (2005) ARL1, a LOB-domain protein required for adventitious root formation in rice. *The Plant Journal*, **43**(1), 47–56. Available from: https://doi.org/10.1111/j.1365-313X.2005.02434.x

Luo, Y., **Teng, S.**, **Yin, H.**, **Zhang, S.**, **Tuo, X.** & **Tran, L.P.** (2021) Transcriptome analysis reveals roles of anthocyanin- and jasmonic acid-biosynthetic pathways in rapeseed in response to high light stress. *International Journal of Molecular Sciences*, **22**(23), 13027. Available from: https://doi.org/10.3390/ijms222313027

Mähönen, A.P., **Ten Tusscher, K.**, **Siligato, R.**, **Smetana, O.**, **Díaz-Triviño, S.**, **Salojärvi, J.** ***et al.*** (2014) PLETHORA gradient formation mechanism separates auxin responses. *Nature*, **515**(7525), 125–129. Available from: https://doi.org/10.1038/nature13663

Mao, C., **He, J.**, **Liu, L.**, **Deng, Q.**, **Yao, X.**, **Liu, C.** ***et al.*** (2020) OsNAC2 integrates auxin and cytokinin pathways to modulate rice root development. *Plant Biotechnology Journal*, **18**(2), 429–442. Available from: https://doi.org/10.1111/pbi.13209

Marhava, P., **Hoermayer, L.**, **Yoshida, S.**, **Marhavý, P.**, **Benková, E.** & **Friml, J.** (2019) Re-activation of stem cell pathways for pattern restoration in plant wound healing. *Cell*, **177**(4), 957–969.e13. Available from: https://doi.org/10.1016/j.cell.2019.04.015

Nguyen, T.N., **Tuan, P.A.**, **Mukherjee, S.**, **Son, S.** & **Ayele, B.T.** (2018) Hormonal regulation in adventitious roots and during their emergence under waterlogged conditions in wheat. *Journal of Experimental Botany*, **69**(16), 4065–4082. Available from: https://doi.org/10.1093/jxb/ery190

Pieterse, C.M., **Van der Does, D.**, **Zamioudis, C.**, **Leon-Reyes, A.** & **Van Wees, S.C.** (2012) Hormonal modulation of plant immunity. *Annual Review of Cell and Developmental Biology*, **28**, 489–521. Available from: https://doi.org/10.1146/annurev-cellbio-092910-154055

Rasmussen, C.G. & **Bellinger, M.** (2018) An overview of plant division-plane orientation. *The New Phytologist*, **219**(2), 505–512. Available from: https://doi.org/10.1111/nph.15183

Rogowska, A., **Stpiczyńska, M.**, **Pączkowski, C.** & **Szakiel, A.** (2022) The influence of exogenous jasmonic acid on the biosynthesis of steroids and triterpenoids in *Calendula officinalis* plants and hairy root culture. *International Journal of Molecular Sciences*, **23**(20), 12173. Available from: https://doi.org/10.3390/ijms232012173

Roychoudhry, S. & **Kepinski, S.** (2022) Auxin in root development. *Cold Spring Harbor Perspectives in Biology*, **14**(4), a039933. Available from: https://doi.org/10.1101/cshperspect.a039933

Saniewski, M., **Ueda, J.** & **Miyamoto, K.** (2002) Relationships between jasmonates and auxin in regulation of some physiological processes in higher plants. *Acta Physiologiae Plantarum*, **24**(2), 211–220. Available from: https://doi.org/10.1007/s11738-002-0013-9

Singh, S.R., **Singh, R.**, **Kalia, S.**, **Dalal, S.**, **Dhawan, A.K.** & **Kalia, R.K.** (2013) Limitations, progress and prospects of application of biotechnological

tools in improvement of bamboo-a plant with extraordinary qualities. *Physiology and Molecular Biology of Plants*, **19**(1), 21–41. Available from: https://doi.org/10.1007/s12298-012-0147-1

Singh, Z., **Singh, H.**, **Garg, T.**, **Mushahary, K.K.K.** & **Yadav, S.R.** (2023) Genetic and hormonal blueprint of shoot-borne adventitious root development in rice and maize. *Plant & Cell Physiology*, **63**(12), 1806–1813. Available from: https://doi.org/10.1093/pcp/pcac084

Steffens, B. & **Rasmussen, A.** (2016) The physiology of adventitious roots. *Plant Physiology*, **170**(2), 603–617. Available from: https://doi.org/10.1104/pp.15.01360

To, H.T.M., **Pham, D.T.**, **Le Thi, V.A.**, **Nguyen, T.T.**, **Tran, T.A.**, **Ta, A.S.** ***et al.*** (2022) The Germin-like protein OsGER4 is involved in promoting crown root development under exogenous jasmonic acid treatment in rice. *Plant Journal*, **112**(3), 860–874. Available from: https://doi.org/10.1111/tpj.15987

Verstraeten, I., **Schotte, S.** & **Geelen, D.** (2014) Hypocotyl adventitious root organogenesis differs from lateral root development. *Frontiers in Plant Science*, **5**, 495. Available from: https://doi.org/10.3389/fpls.2014.00495

Wan, Q., **Yao, R.**, **Zhao, Y.** & **Xu, L.** (2025) JA and ABA signaling pathways converge to protect plant regeneration in stress conditions. *Cell Reports*, **44**(3), 115423. Available from: https://doi.org/10.1016/j.celrep.2025.115423

Wang, R., **Wang, Y.**, **Yao, W.**, **Ge, W.**, **Jiang, T.** & **Zhou, B.** (2023) Transcriptome sequencing and WGCNA reveal key genes in response to leaf blight in poplar. *International Journal of Molecular Sciences*, **24**(12), 10047. Available from: https://doi.org/10.3390/ijms241210047

Wang, S., **Pei, J.**, **Li, J.**, **Tang, G.**, **Zhao, J.**, **Peng, X.** ***et al.*** (2020) Sucrose and starch metabolism during *Fargesia yunnanensis* shoot growth. *Physiologia Plantarum*, **168**(1), 188–204. Available from: https://doi.org/10.1111/ppl.12934

Wang, S., **Yang, N.**, **Pu, X.**, **Li, F.** & **Ding, Y.** (2010) A preliminary study on cutting propagation of *Fargesia yunnanensis*. *Journal of Bamboo Research*, **29**(3), 31–34. (in Chinese).

Weiszmann, J., **Fürtauer, L.**, **Weckwerth, W.** & **Nägele, T.** (2018) Vacuolar sucrose cleavage prevents limitation of cytosolic carbohydrate metabolism and stabilizes photosynthesis under abiotic stress. *The FEBS Journal*, **285**(21), 4082–4098. Available from: https://doi.org/10.1111/febs.14656

Yamauchi, T., **Watanabe, K.**, **Fukazawa, A.**, **Mori, H.**, **Abe, F.**, **Kawaguchi, K.** ***et al.*** (2014) Ethylene and reactive oxygen species are involved in root aerenchyma formation and adaptation of wheat seedlings to oxygen-deficient conditions. *Journal of Experimental Botany*, **65**(1), 261–273. Available from: https://doi.org/10.1093/jxb/ert371

Yan, C., **Fan, M.**, **Yang, M.**, **Zhao, J.**, **Zhang, W.**, **Su, Y.** ***et al.*** (2018) Injury activates Ca^{2+}/calmodulin-dependent phosphorylation of JAV1-JAZ8-WRKY51 complex for jasmonate biosynthesis. *Molecular Cell*, **70**(1), 136–149.e7. Available from: https://doi.org/10.1016/j.molcel.2018.03.013

Yang, D.L., **Yao, J.**, **Mei, C.S.**, **Tong, X.H.**, **Zeng, L.J.**, **Li, Q.** ***et al.*** (2012) Plant hormone jasmonate prioritizes defense over growth by interfering with gibberellin signaling cascade. *Proceedings of the National Academy of Sciences of the United States of America*, **109**(19), E1192–E1200. Available from: https://doi.org/10.1073/pnas.1201616109

Yang, L., **Xu, L.**, **Guo, J.**, **Li, A.**, **Qi, H.**, **Wang, J.** ***et al.*** (2024) SNAC1-OsERF103-OsSDG705 module mediates drought response in rice. *New Phytologist*, **241**(6), 2480–2494. Available from: https://doi.org/10.1111/nph.19552

Yoon, J., **Cho, L.H.**, **Tun, W.**, **Jeon, J.S.** & **An, G.** (2021) Sucrose signaling in higher plants. *Plant Science*, **302**, 110703. Available from: https://doi.org/10.1016/j.plantsci.2020.110703

Yu, F., **Liang, K.**, **Fang, T.**, **Zhao, H.**, **Han, X.**, **Cai, M.** ***et al.*** (2019) A group VII ethylene response factor gene, ZmEREB180, coordinates waterlogging tolerance in maize seedlings. *Plant Biotechnology Journal*, **17**(12), 2286–2298. Available from: https://doi.org/10.1111/pbi.13140

Yu, L., **Pei, J.**, **Zhao, Y.** & **Wang, S.** (2021) Physiological changes of bamboo (*Fargesia yunnanensis*) shoots during storage and the related cold storage mechanisms. *Frontiers in Plant Science*, **12**, 731977. Available from: https://doi.org/10.3389/fpls.2021.731977

Zeng, J., **Zhang, T.**, **Huangfu, J.**, **Li, R.** & **Lou, Y.** (2021) Both allene oxide synthases genes are involved in the biosynthesis of herbivore-induced jasmonic acid and herbivore resistance in rice. *Plants (Basel)*, **10**(3), 442. Available from: https://doi.org/10.3390/plants10030442

Zhao, Z., **Zhang, Z.**, **Ding, Z.**, **Meng, H.**, **Shen, R.**, **Tang, H.** ***et al.*** (2020) Public-transcriptome-database-assisted selection and validation of reliable reference genes for qRT-PCR in rice. *Science China. Life Sciences*, **63**(1), 92–101. Available from: https://doi.org/10.1007/s11427-019-1553-5

Zhou, W., **Lozano-Torres, J.L.**, **Blilou, I.**, **Zhang, X.**, **Zhai, Q.**, **Smant, G.** ***et al.*** (2019) A jasmonate signaling network activates root stem cells and promotes regeneration. *Cell*, **177**(4), 942–956.e14. Available from: https://doi.org/10.1016/j.cell.2019.03.006

Zhu, C., **Gan, L.**, **Shen, Z.** & **Xia, K.** (2006) Interactions between jasmonates and ethylene in the regulation of root hair development in Arabidopsis. *Journal of Experimental Botany*, **57**(6), 1299–1308. Available from: https://doi.org/10.1093/jxb/erj103